

Obtaining Smoothly Navigable Approximation Sets in Bi-Objective Multi-Modal Optimization

Renzo J. Scholman*
Centrum Wiskunde & Informatica
Amsterdam, The Netherlands
Renzo.Scholman@cwi.nl

Anton Bouter
Centrum Wiskunde & Informatica
Amsterdam, The Netherlands
Anton.Bouter@cwi.nl

Leah R.M. Dickhoff
Leiden University Medical Center
Leiden, The Netherlands
L.R.M.Dickhoff@lumc.nl

Tanja Alderliesten
Leiden University Medical Center
Leiden, The Netherlands
T.Alderliesten@lumc.nl

Peter A.N. Bosman*
Centrum Wiskunde & Informatica
Amsterdam, The Netherlands
Peter.Bosman@cwi.nl

ABSTRACT

Even if a Multi-modal Multi-Objective Evolutionary Algorithm (MMOEA) is designed to find all locally optimal approximation sets of a Multi-modal Multi-objective Optimization Problem (MMOP), there is a risk that the found approximation sets are not smoothly navigable because the solutions belong to various niches, reducing the insight for decision makers. Moreover, when the multi-modality of MMOPs increases, this risk grows and the trackability of finding all locally optimal approximation sets decreases. To tackle these issues, two new MMOEAs are proposed: Multi-Modal Bézier Evolutionary Algorithm (MM-BezEA) and Set Bézier Evolutionary Algorithm (Set-BezEA). Both MMOEAs produce approximation sets that cover individual niches and exhibit inherent decision-space smoothness as they are parameterized by Bézier curves. MM-BezEA combines the concepts behind the recently introduced BezEA and MO-HillValleEA to find all locally optimal approximation sets. Set-BezEA employs a novel multi-objective fitness function formulation to find limited numbers of diverse, locally optimal, approximation sets for MMOPs of high multi-modality. Both algorithms, but especially MM-BezEA, are found to outperform the MMOEAs MO_Ring_PSO_SCD and MO-HillValleEA on MMOPs of moderate multi-modality with linear Pareto sets. Moreover, for MMOPs of high multi-modality, Set-BezEA is found to indeed be able to produce high-quality approximation sets, each pertaining to a single niche.

CCS CONCEPTS

• **Mathematics of computing** → **Evolutionary algorithms.**

KEYWORDS

Evolutionary algorithms, multi-modal multi-objective optimization, niching, Bézier curve estimation

1 INTRODUCTION

Many real-world optimization problems have multiple conflicting objectives, whereby improvement in one objective often results in the deterioration of another. Multi-Objective Evolutionary Algorithms (MOEAs), like the Multi-Objective Real-Valued Gene-pool Optimal Mixing (MO-RV-GOMEA) [9] algorithm, are widely accepted to be well-suited to solve such Multi-objective Optimization

*Also with Delft University of Technology, Delft, The Netherlands.

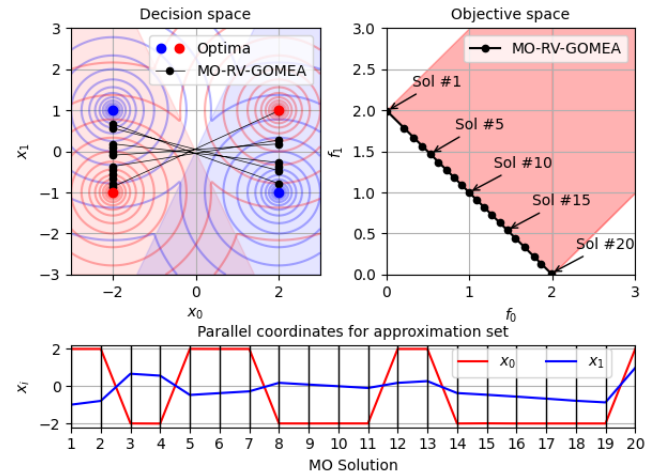


Figure 1: Approximation set and front with parallel coordinates plot as produced by MO-RV-GOMEA on MinDist problem, where $f_0(x) = \min(\|x - [1, -1]\|, \|x - [-1, 1]\|)$ and $f_1(x) = \min(\|x - [1, 1]\|, \|x - [-1, -1]\|)$. Shaded blue and red regions correspond to niches with global PSs.

Problems (MOPs) [12]. The aim is to obtain a set of solutions, called the approximation set, such that all solutions are non-dominated and the set itself is close to the set of Pareto-optimal solutions.

A more complex type of MOPs is that of Multi-modal MOPs (MMOPs), where the goal is not to find one, but multiple, if not all, (local) Pareto sets (PSs). Each of these pertains to a *niche*, a subset of the search space, where a single mode resides. The PSs may, however, well map to the same Pareto Front (PF) in objective space, similar to having multiple (locally) optimal solutions of the same quality in a single-objective problem, e.g., the sine function.

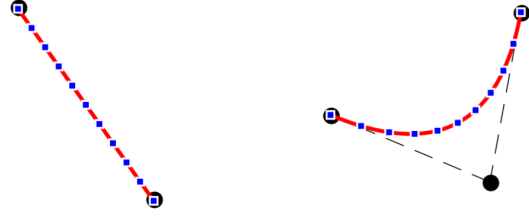
In order to have MOEAs solve MMOPs, they need additional tools that prevent their convergence to a single niche of the landscape [22]. Niching [20] is one of many diversity-preserving tools used by Multi-modal MOEAs (MMOEA) to effectively and simultaneously search for solutions near the (local) PS in each niche. Niching has been successfully applied to established MMOEA in the form of the multi-objective particle swarm optimization using ring topology and special crowding distance (MO_Ring_PSO_SCD) algorithm [34] and Omni-optimizer [13] among others.

Most MMOEAs do not explicitly model multiple approximation sets, but include diversity preserving techniques to ensure that solutions from multiple niches are maintained. The result of these MMOEAs is usually given in the form of a single approximation front, often derived from (a subset of) the elitist archive. A decision maker can then investigate this front by traversing the solutions for desired trade-offs. However, the underlying solutions are taken from several distinct niches. This results in observing a counter-intuitive change in decision variable values when navigating the approximation front. Figure 1 shows such an approximation front and set that contains solutions from both modes on the MinDist problem [23] and demonstrates the counterintuitive changes in decision variable values in the parallel coordinates plot (i.e., if one were to traverse the front and inspect solutions). It shows that in objective space a front is found that looks to have approximated the PF to (near) optimality, but the solutions jump around throughout decision space. Especially in highly multi-modal problems, solutions can originate from many different modes, which may make it more insightful for decision makers to be able to request approximation sets for a specific number of modes.

The issue of counterintuitive navigation along the approximation front has also been explored in recent works, which introduced a new indicator-based MOEA for bi-objective optimization called BezEA [24]. A new problem formulation for population-based MOEAs was introduced whereby they parameterized approximation sets as Bézier curves. This ensured the navigational smoothness of an approximation set, whilst still being able to find good approximation sets when using the HyperVolume indicator (HV) [36]. By design, BezEA disallowed curves to dominate parts of themselves to ensure that the approximation set constitutes a single niche in the landscape.

Recent work that included the concept of niching showed promising results in maintaining multiple approximation sets in a population-based MMOEAs called the MO-HillValLEA [23]. The authors extended the concept of Hill-Valley Clustering (HVC) [26] for MOPs to Multi-Objective HVC (MO-HVC) for MMOPs. It is capable of finding and preserving approximation sets, one for each niche, in parallel over time by considering Pareto domination per niche. However, MO-HillValLEA produces approximation sets that are not inherently smooth due to slight oscillation around the PS. Furthermore, no limit on the number of approximation sets can be set, which degrades the quality of the approximation sets in highly multi-modal problems as the population is divided over all niches.

In this work, the notions of niching through HVC and Bézier curve parameterizations will be combined. The use of niching allows to effectively search the multi-modal landscape. Whereas the use of Bézier curve parameterizations not only enforces the smooth and intuitive navigability that is desired by decision makers, but also enforces each approximation set to be within a single niche. Furthermore, the use of the HV indicator allows the new algorithms to converge closer to the PS as compared to the Pareto dominance-based algorithms [5]. Two new algorithms are proposed that combine the aforementioned techniques, called Multi-Modal Bézier Evolutionary Algorithm (MM-BezEA) and Set Bézier Evolutionary Algorithm (Set-BezEA). These respectively try to find all approximation sets for a given MMOP or a specific number of



$B(t; C_2) = (1-t)c_1 + tc_2$ $B(t; C_3) = (1-t)^2c_1 + 2(1-t)tc_2 + t^2c_3$
Figure 2: Bézier curves with $q \in 2, 3$ control points in black. In red is the interpolated curve with in blue the $p = 11$ points evenly spread in the domain of t along the curve. [24]

approximation sets for MMOPs that are highly multi-modal, where each approximation set consists of solutions from a single mode.

In order to combine the techniques of Bézier curve parameterizations and HVC into the two proposed new algorithms, several contributions are made. First, the problem of how to niche approximation sets in the form of Bézier curve parameterizations is resolved. Second, initialization of approximation sets within a single niche is enabled, as otherwise, clustering becomes ambiguous if they span multiple niches. Last, a new fitness function formulation is introduced to find a preset number of approximation sets for highly multi-modal problems.

2 BÉZIER PARAMETERIZATIONS

One of the key features of the newly proposed algorithms is that Bézier parameterizations are used as approximation sets for bi-objective optimization [24]. This allows the algorithm to model the approximation set as a smooth curve through decision space.

2.1 Definition of solution set

An ℓ -dimensional Bézier curve $B(t; C_q)$ can be defined using $q \geq 2$ control points c_i in an ordered set $C_q = \{c_1, \dots, c_q\}$, where ℓ is the problem dimensionality and $c_i \in \mathbb{R}^\ell$. The full notation is:

$$B(t; C_q) = \sum_{i=1}^q \binom{q-1}{i-1} (1-t)^{q-i-1} t^{i-1} c_i \text{ for } 0 \leq t \leq 1 \quad (1)$$

The endpoints of the Bézier curve are always defined by the first and last control points, whilst the other control points are normally not located on the curve. A solution set of given size p , $S_{p,q}(C_q) = \{x_1, \dots, x_p\}$ with $x_i \in \mathbb{R}^\ell$, can now be parameterized by a Bézier curve by selecting an evenly spread set of p points x_i . Figure 2 visualizes two solution sets $S_{p,q}(C_q)$ parameterized by Bézier curves. The solution set $S_{p,q}(C_q)$ is formally defined as:

$$S_{p,q}(C_q) = \left\{ B\left(\frac{0}{p-1}; C_q\right), B\left(\frac{1}{p-1}; C_q\right), \dots, B\left(\frac{p-1}{p-1}; C_q\right) \right\} \quad (2)$$

$S_{p,q}(C_q)$ is parameterized for (M)MOEAs by taking the concatenation of the decision variables in the set C_q as a solution [6, 24]. This results in a solution being of the form $[c_1, \dots, c_q] \in \mathbb{R}^{q*\ell}$.

2.2 Evaluation

To evaluate a solution set $S_{p,q}(C_q)$, a number of new functions were previously introduced [24]. These functions are briefly explained in the following paragraphs. Figure 3 illustrates these functions to give the reader a more graphical indication.

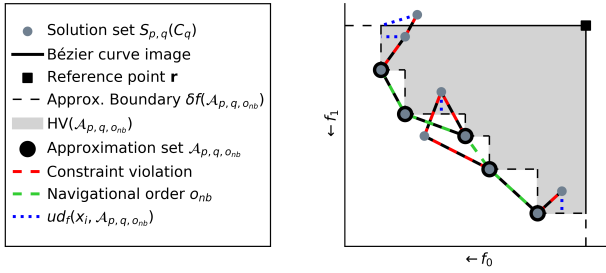


Figure 3: Evaluation of Bézier parameterizations. [24]

A new function $A^{nb}(S_{p,q})$ has been introduced that calculates a navigational Bézier (nb) order o_{nb} . This order is defined as starting from the best solution for objective f_0 to the best solution in f_1 . All solutions that are dominated by others, which lie on the curve, are omitted from the subset that defines the navigational order. An approximation set $\mathcal{A}_{p,q,o_{nb}}$ is then the resulting subset of $S_{p,q}(C_q)$. The quality of the approximation set $\mathcal{A}_{p,q,o_{nb}}$ can now be evaluated, e.g., using the uncrowded HV indicator [25].

A new constraint function $C(S_{p,q,o_{nb}})$ was also introduced. It is employed in order to not only push all dominated solutions on the curve towards the undominated region of the search space, but also to prevent the curve from wrapping around itself in objective space. This may for instance happen if a curve stretches across two local PSs, which is not preferential. The constraint function uses the uncrowded distance metric $ud_f(x_i, \mathcal{A})$ [32], which measures the Euclidean distance from a dominated point x_i to the approximation boundary $\delta f(\mathcal{A}_{p,q,o_{nb}})$ in objective space. Furthermore, to further increase pressure towards the unfolding of Bézier curves in objective space, all dominated solutions and those not in $\mathcal{A}_{p,q,o_{nb}}$ are pulled towards their neighbouring solutions on the Bézier curve by taking the Euclidean distance in objective space between these solution and their neighbours as an additional constraint value. All dominated solutions from $S_{p,q}(C_q)$ now have their uncrowded distance values and the Euclidean distances in objective space to neighbours of those not in $\mathcal{A}_{p,q,o_{nb}}$ summed up as a constraint for the total solution set. In combination with constraint domination [11], this constraint pushes all solutions along the Bézier curve towards the undominated region.

3 NICHING METHODS

To allow the two algorithms proposed in this paper, i.e., MM-BezEA and Set-BezEA, to effectively search the multi-modal landscape, several previously introduced niching methods are used and combined. These are employed in order to extend on the uni-modal search that is originally performed by BezEA. As the number of modes is usually unidentified beforehand, the algorithms need to be able to adapt to the number of modes present in an MMOP, or the number a user is after.

3.1 HVC and MO HVC

HVC is a so-called two-stage niching approach that clusters and evolves the population for multi-modal single-objective optimization problems. In each generation, the first stage is used to locate

each of the distinct niches, for each of which a core search algorithm is initialized in the second stage.

At the heart of the HVC approach is the Hill-Valley Test (HVT) [33], which can be utilized to determine whether two solutions reside in the same niche. This test first determines an edge between two solutions x_i and x_j in the search space. Along this edge, N_t evenly spread points are evaluated, determined by the distance between the two solutions divided by the expected edge length. If any of these N_t test points have a fitness that is worse than that of x_i and x_j , the test detects that there is a *hill* in between them. Consequently, the two solutions are to be put in separate clusters. On the other hand, if all N_t points have equal or better fitness values than both x_i and x_j , these two solutions belong to the same *valley* and are to be clustered together. A pseudocode example of this test can be found in Algorithm 1.

Algorithm 1: [Boolean] = HillValleyTest(x_i, x_j, N_t, f) [33]

Input: Solutions $x_i, x_j, N_t \in \mathbb{Z}$, objective function f

for $k = 1, \dots, N_t$ **do**

$$x_{test} = x_i + \frac{k}{N_t + 1} (x_j - x_i)$$

if $\max\{f(x_i), f(x_j)\} < f(x_{test})$ **then return false**

return true

In order to determine in which order the solutions are to be clustered (i.e., undergo the HVT), the concept of the nearest better tree [27] is employed. It sorts the solutions in descending order of fitness, whereby the first solution automatically forms the first cluster. Then, the population is traversed in this descending order, starting at the second best solution, and each solution x_i is tested with the HVT to decide if it belongs to the same cluster as its nearest better neighbour x_j . If the test returns false, it is repeated at most $\ell + 1$ times with the next-nearest better neighbours x_j , before concluding that the solution x_i belongs to a new cluster.

The MO-HillValleEA algorithm [23] expands on the previous HVC approach in the form of MO-HVC. It uses the same concept of the HVT, but now performs clustering for each of the m objective functions separately, which results in m cluster sets of the population. To obtain a single cluster set, the intersection of all clustering sets is taken, similar to the colored regions of Figure 1.

3.2 Restart scheme with elitist archive

Various algorithms implemented a form of a restart scheme whereby the population size is increased over time. Examples of such schemes are the interleaved multistart scheme [9] and the restart-Covariance Matrix Adaptation Evolution Strategy with Increased Population (IPOP-CMA-ES) algorithm [4]. In HillValleEA [26], an elitist archive is combined with a restart scheme, where the population size is doubled after each restart as in IPOP-CMA-ES [4]. By employing the HVT to check if a solution resides in another niche, the elitist archive of HillValleEA is capable of holding the elites for each of the modes, despite it being developed for single objective problems.

To prevent HillValleEA from revisiting already searched modes, it makes use of the elitist archive, which is inspired by the repelling subpopulations (RS-CMSA) algorithm [1] that defines taboo regions close to elites. The steps taken to discard the regions of the search

space, for which an elite was already found in one of the earlier populations, start with adding the elites to the population of the current restart. Then, all solutions are clustered using HVC, followed by discarding all clusters that have one of the elites as their best solution. As a result of discarding these regions of the search space, more attention is given to undiscovered parts of the search space after each restart.

3.3 Fitness sharing

Fitness sharing [18] is another niching technique aimed at keeping the population diverse. It does so by degrading certain individuals fitness values if these solutions are close to one another. This is to be done using a niche radius parameter σ_{share} defining which solutions are close, together with a scaling factor α that degrades the fitness [15]. However, it has been shown non-trivial to set correct values for these parameters [10].

4 MULTI MODAL-BÉZIER EVOLUTIONARY ALGORITHM

In this section the Multi-Modal Bézier Evolutionary Algorithm, abbreviated as MM-BezEA, is described. It has been created through the combination and modification of techniques described in the previous sections. The most notable of the modifications are the adjustments implemented in HVC in order to apply it to Bézier curve parameterizations, as well as the initialization of approximation sets within niches.

4.1 Clustering approximation sets

The Bézier curves are evaluated using the uncrowded HV measure [25]. Since this is a scalar, the HVC approach is essentially applicable in a rather straightforward manner because it intuitively allows the clustering of single-objective problems. However, the approximation set $\mathcal{A}_{p,q,o_{nb}}$ that is used in the HV calculation only considers the undominated indices of the Bézier solution set $S_{p,q}(C_q)$ as defined in o_{nb} . Hence, the objective value given to the solution set $S_{p,q}(C_q)$ seems highly dependent on how many dominated solutions there are on the Bézier curve.

To enable the clustering of Bézier solution sets $S_{p,q}(C_q)$, the idea behind MO-HVC can be used on the set of control points C_q because each of these is a single solution as normally defined in MO optimization. Also, since a solution set is defined to be deteriorating in f_0 and improving in f_1 according to o_{nb} , the order of the control points is inverted if $f_0(c_1) < f_0(c_q)$ does not hold [24]. Accordingly, the i -th Bézier solution can be designated to be in the same niche as

Algorithm 2: $[B] = \text{Bezier-HillValleyTest}(S_i, S_j, N_t, f)$

Input: Solutions sets S_i, S_j , int N_t , objective functions f_0, \dots, f_{m-1}

Output: Whether S_i and S_j belong to the same niche

```

for  $l = 1, \dots, q$  do
   $c_{i,l} =$  control point  $l$  of  $S_i$ 
   $c_{j,l} =$  control point  $l$  of  $S_j$ 
  // check  $c_{i,l}$  and  $c_{j,l}$  are in same niche for all  $m$  objectives
  for  $k = 0, \dots, m - 1$  do
    | if  $\text{HillValleyTest}(c_{i,l}, c_{j,l}, N_t, f_k)$  then return false
return true

```

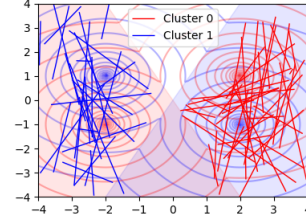


Figure 4: Initialization of Bézier solutions ($q = 2$) for MinDist.

the j -th Bézier solution if their control points $c_l^i \in C_q^i$ and $c_l^j \in C_q^j$ for $l = \{1, \dots, q\}$ are in the same niche. In a general sense, the same HVC approach as used in HillValLEA is used, but inspiration has been taken from the MO-HVC approach to produce a new test for Bézier solution sets, which is shown in Algorithm 2.

4.2 Initialization within niches

The original BezEA algorithm initializes all solution sets by sampling from a uniform distribution over the search space. As it is an MOEA that was not designed for multi-modal optimization, the uniform initialization allows solution sets to be initialized within or in between any niche(s). Clustering these solutions with the newly introduced Bézier HVT will result in finding a large number of separate niches as each control point has to be in the same mode.

To prevent this, a new initialization method for Bezier solution sets is proposed to enforce their initialization within a niche. First, an iteration of MO-HVC is run on a set of $q * N$ solutions, N being the population size, that is sampled from a uniform distribution over the search space, where the resulting clusters include all of the x_{test} solutions resulting from applying Algorithm 1. Second, selection is performed on the clusters proportional to their size in order to reduce their combined size, with test solutions, down to $q * N$. Lastly, Bézier solution sets $S_{p,q}(C_q)$ are initialized by randomly choosing q solutions as the control points from one single cluster C as produced by MO-HVC. A visualization of the result can be seen in Figure 4.

4.3 Algorithm overview

MM-BezEA has a similar structure as the restart scheme in HillValLEA [26] that is described in section 3.2. Every iteration, the combination of taboo regions and subsequent initialization of Bézier curves takes place. For each of the resulting niches, a core search algorithm is run for one generation, which in the case of MM-BezEA is the RV-GOMEA algorithm [8] that is also used in BezEA. At the end of each generation, the Bézier HVT of Algorithm 2 is used in the HVC step. This step takes all solutions originating from all clusters and clusters them again for the next generation. In between generations, the notion of cluster registration [7] is used on the cluster mean closest in decision space to transfer the parameters for RV-GOMEA between the clusters of each generation. An overview of the algorithm in the form of pseudocode is given in Algorithm 3.

Algorithm 3: $[\mathbb{E}] = \text{MM-BezEA}(f, N, p, q)$

Input: MO function f , population size N , number of test points p , number of control points q , evaluation or runtime budget

Output: Elitist archive $\mathbb{E} = [\mathcal{E}_0, \mathcal{E}_1, \dots]$

$\mathcal{P}_{mo} = \text{UniformSampling}(q \cdot N, f)$

$\mathbb{C}_{mo} = \text{MO-HillValleyClustering}(\mathcal{P}_{mo}, f)$

$\mathbb{C} = \text{InitializeBezierSolutions}(\mathbb{C}_{mo}, q, p, f)$

$\mathbb{E} = \text{InitializeElitistArchive}(\mathbb{C})$

while budget remaining **do**

$\mathcal{P} = \mathbb{E}$

for $C_i \in \mathbb{C}$ **do**

$O_i = \text{core_search_algorithm}(C_i)$

$\mathcal{P} = \mathcal{P} \cup O_i$

$\mathbb{C}_{prev} = \mathbb{C}$

$\mathbb{C} = \text{BezierHillValleyClustering}(\mathcal{P}, f)$

$\mathbb{E} = \text{ConstructElitistArchive}(\mathbb{C}, \mathbb{E})$

$\mathbb{C} = \text{RemoveElitesFrom}(\mathbb{C})$

$\mathbb{C} = \text{ClusterRegistration}(\mathbb{C}, \mathbb{C}_{prev})$

5 SET BÉZIER EVOLUTIONARY ALGORITHM

As MM-BezEA is a niching method that divides its attention over all of the niches found by HVC, it is intractable to use MM-BezEA in highly multi-modal landscapes. In order to overcome this limitation, a second algorithm is introduced that uses MO-RV-GOMEA [9] with an adapted fitness function definition and encoding. Rather than encoding each solution to be one Bézier curve, and clustering the population to find different niches, this algorithm, named Set-BezEA, encodes and searches for a set of b Bézier curves. It does so without further niching the population, which prevents this approach from falling apart in highly multi-modal landscapes.

In the original BezEA, solutions represent Bézier curves consisting of the q control points C_q . Given a problem dimensionality ℓ , a Bézier solution thus consists of $q \cdot \ell$ parameters. In Set-BezEA, a solution represents b Bézier curves consisting of $b \cdot q$ control points C_q concatenated into a set of control points denoted as $C_{q,b}$. The control points for the i -th Bézier solution are denoted as $C_{q,b}^i$. Hence, solutions in Set-BezEA take the form $[C_{q,b}^1, \dots, C_{q,b}^b] \in \mathbb{R}^{b \cdot q \cdot \ell}$. The notation $S_{p,q}^i$, equal to the definition of $S_{p,q}$ in Equation 2, is used to denote the i -th Bézier solution of the set $S_{p,q,b}$ with b Bézier solutions.

5.1 Fitness function formulation

In order to evaluate the newly formulated solutions, a new fitness function is proposed that can be seen in mathematical form in Equation 3. The original fitness function formulation from BezEA is used in order to determine the constraint $L(S_{p,q,b}(\phi))$ and $\text{HV}_{f,S_{p,q,b}(\phi)}$ values for all of the b Bézier solutions combined. Fitness sharing [18] is incorporated with a niching radius based on the expected edge length [26], which is checked between each of the b Bézier solutions $S_{p,q}^i$.

However, fitness sharing only describes a minimal separation criterion. Typically, in practice, decision makers would like to be able to find Bézier solutions that are diverse, yet all of high quality, while limited in number. For this reason, the problem is defined as an MO formulation. Herein, the second objective is a distance objective

$$\begin{aligned} \text{maximize } f_0: \quad \text{HV}_{f,S_{p,q,b}(\phi)} &= \sum_{i=0}^{b-1} \frac{\text{HV}_f \left(A^{nb} \left(S_{p,q}^i(\phi) \right) \right)}{n_i} \\ \text{maximize } f_1: \quad \Delta_{S_{p,q,b}(\phi)} &= \sum_{i=0}^{b-1} \sum_{j=i+1}^{b-1} \frac{S_{p,q}^i(\phi) \cdot S_{p,q}^j(\phi)}{\|S_{p,q}^i(\phi)\| \|S_{p,q}^j(\phi)\|} \quad (3) \\ \text{with constraint: } L(S_{p,q,b}(\phi)) &= \sum_{i=0}^{b-1} L_b \left(S_{p,q}^i(\phi), o_{nb}^i(\phi) \right) \end{aligned}$$

where $f: \mathbb{R}^\ell \rightarrow \mathbb{R}^m$, $\phi \in \mathbb{R}^{b \cdot q \cdot \ell}$,

A^{nb} : solution set $S_{p,q}^i(\phi) \rightarrow$ approximation set $\mathcal{A}_{p,q,o_{nb}}^i$

n_i number of Bézier curves in same niche as $S_{p,q}^i$

$o_{nb}^i(\phi)$ the navigational order of the i -th Bézier solution

$L_b(S_{p,q}^i(\phi), o_{nb}^i(\phi))$ the Bézier constraint function

$\Delta_{S_{p,q,b}}$ that is to be maximized. It calculates the sum of cosine distances between all pairs of the b Bézier solutions to move them apart in decision space and promote finding diverse approximation sets.

5.2 Adaptive steering

The MO formulation of the previous section creates a trade-off between finding far apart solutions at the edges of the search space and those closer to the PSs. However, especially assuming the global optimum cannot be obtained, the primary goal is to obtain distinct solutions that are of high quality. Most (M)MOEAs try to find improvements spread over the entire PF, whereas in some situation only a part of the PF is interesting. In order to steer Set-BezEA towards the interesting parts of the PF, the notion of adaptive steering [2] can be used on the first objective value. Starting at allowing Bézier set solutions to be within 50% of the best achieved cumulative HV it scales linearly in 50 generations to 99%. This will force all solutions towards higher HV values when combined with constraint domination [11].

5.3 Linkage structure and partial evaluations

To optimize for the new fitness formulation, Set-BezEA uses MO-RV-GOMEA, which uses a linkage model [30] to determine which variables are to be changed at the same time. It is often taken to be a linkage tree that is constructed using the unweighted pair group method with arithmetic mean (UPGMA) [16] to iteratively cluster decision variables. A new linkage structure is designed for Set-BezEA to guide MO-RV-GOMEA and allow it to exploit the underlying structure of a problem. For this new linkage structure, the ideas behind the linkage structures defined for BezEA and UHV-GOMEA were combined [24].

When the j -th decision variable of a control point in Bézier curve changes, the j -th decision variable of all test solutions of the approximation set $S_{p,q}^i(C_q)$ changes, which makes it beneficial to change the same decision variable for all q control points of a Bézier curve at once. This is the first layer of the new linkage structure, where, for each of the b Bézier solutions, their j -th decision variables of all q control points are grouped. Subsequently, the ℓ clusters of q decision variables for one Bézier solution are hierarchically grouped using UPGMA. The second layer combines the b resulting groups

of the decision variables of all b Bézier solutions by concatenating them into one large linkage tree.

The newly defined linkage structure enables MO-RV-GOMEA to perform partial evaluations in all situations. Even if the underlying problem setting is black-box in nature, partial evaluations are enabled by the second layer, as each of these Bézier curves can be evaluated separately for its HV contribution to the first objective. The second distance objective always has to be recalculated, but it does not require any evaluations of the original fitness function.

5.4 MO-RV-GOMEA adaptations

The approximation sets $S_{p,q}^i(C_q)$, defined by the Bézier curves, are evaluated with the HV indicator that makes use of a reference point. But, the choice of reference point highly influences whether or not the extremes of the PF can be found [3].

The control points c_1^i and c_q^i are likely to come as close as possible to the constraint region, defined by being dominated by the reference point, to maximize the HV. However, if one of these two control points falls just slightly in the constraint region, the constraint function $C(S_{p,q,b}(\phi))$ combined with constraint domination will make it one of the worst performing solutions. Furthermore, MO-RV-GOMEA makes use of the Gene-pool Optimal Mixing (GOM) variation operator, thereby disallowing deterioration of fitness. These two effects combined, quickly reduce the variance in the population, since very slight adjustments can significantly deteriorate the individual. In order to overcome this downside, the GOM part of MO-RV-GOMEA has been adapted to allow deterioration of the objective values, i.e., accepting a modification that would otherwise have been rejected, with a probability of 5%, as was previously done in RV-GOMEA [8]. This adaptation enables MO-RV-GOMEA to effectively search the outer regions of the search space close to the constraint space by preserving more variance.

6 EXPERIMENTS

MM-BezEA and Set-BezEA are empirically benchmarked on several test problems. The results are compared to MO-HillValLEA [23], MO-RV-GOMEA [9], and MO_Ring_PSO_SCD [34]. MO_Ring_PSO_SCD is implemented through the PlatEMO framework [31], where all of the used metrics and problems are manually implemented as well. For the other algorithms, original C++ implementations are used.

6.1 Test problems

Several test problems are employed. First of these is the MinDist problem [23] that was described in the introduction, where linear PSs are to be found. The other employed functions are frequently used in literature, namely OmniTest [13], Two on One [28], and Sympart {1,2,3} [29]. Lastly, several problems are taken from the Multi-modal Multi-objective test Function (MMF) benchmark suite [21] in the form of MMF {1,2,12,14,15}.

A mix of PS and PF shapes have been chosen to determine the capabilities of the two new algorithms on different problem types. Table 1 shows some of the important characteristics for each of the problems. For all problems with a configurable number of PSs, it is set to 2, likewise the problem dimension ℓ is fixed to 2. In order to determine the values of the performance indicators, the reference

PSs will be made using 5000 points that adhere to the analytical formulas describing the PSs. In the case of Two on One, a very close approximation is used, as no analytical formula is available [28].

6.2 Benchmark setup

In order to get a fair comparison, each of the algorithms will be given an equally sized budget of 200k function evaluations for each of the problems. This removes the influence of the used programming languages, as the computation time is not limited. The parameters of MO-RV-GOMEA, MO_Ring_PSO_SCD, and MO-HillValLEA are set to the values reported in relevant literature. Furthermore, for each problem and metric, the average over 31 runs will be taken.

The elitist archives sizes N_E are set to be 1250 for MO-RV-GOMEA and MO-HillValLEA. The population size N is set to 96 for MO-RV-GOMEA and 250 for MO-HillValLEA. MO-RV-GOMEA uses a linkage tree as its linkage model, with a total of 5 clusters. For MO_Ring_PSO_SCD the population size is 800 [34]. For the MM-BezEA and Set-BezEA algorithms, the number of control points q for each approximation set is set to 2. Just like for the original BezEA algorithm, these two algorithms are both given population sizes of 76 [24]. The number of test points p is set to 7. Lastly, Set-BezEA is always configured to produce $b = 2$ Bézier solutions as approximation sets.

6.3 Performance indicators

The HV indicator [36] is used to see how well the algorithms perform in getting close to the PF. As a result of the use of test points in the MM-BezEA and Set-BezEA algorithms, these algorithms have a limited amount of points in the approximation set that can be used to calculate the HV values. Therefore, a subset of the approximation set will be taken for the other algorithms to allow a fair comparison based on the HV indicator. Specifically, the same number of test points is selected for a fair comparison by means of greedy Hypervolume Subset Selection (gHSS) [17].

We further use a relatively new performance indicator for multi-modal multi objective optimization, named Pareto Set Proximity (PSP) [34]. It is an indicator that determines how well all PSs are approximated by taking the Cover Rate (CR), that shows how well the extremes of all PSs are captured, divided by the Inverted Generational Distance in decision space (IGDX) [35], which can be used to determine how close the approximation sets are to the PSs. For the IGDX measure, the approximation sets as produced by MM-BezEA and Set-BezEA are interpolated by taking 1000 intermediate points before determining the IGDX value. This can be performed

Table 1: Bi-objective problem instances and characteristics.

Problem	ℓ	#PS	PS Shape	PF Shape
MinDist	$[2 \dots \infty) \in \mathbb{Z}$	n	Linear	Convex
Omni Test	$[2 \dots \infty) \in \mathbb{Z}$	3^ℓ	Linear	Convex
Two on One	2	2	Linear	Convex
Sympart 1 & 2	2	9	Linear	Convex
Sympart 3	2	9	Non-linear	Convex
MMF 1 & 2	2	2	Non-linear	Convex
MMF 12	$[2 \dots \infty) \in \mathbb{Z}$	n	Linear	Disconnected
MMF 14 & 15	$[2 \dots \infty) \in \mathbb{Z}$	n	Linear	Concave

relatively easily as interpolating these parameterizations does not require any extra fitness evaluations.

Finally, we use a performance indicator regarding smoothness, for which we follow the definition as introduced in the work on BezEA [24]. It captures how smooth an approximation set can be navigated in terms of decision variables by measuring the detour length in decision space when traversing the approximation set from one solution to the next via an intermediate solution, as compared to going to the next solution directly. The smoothness approaches its maximum value of 1 if all solutions would be colinear in decision space, where the lowest possible value is 0. In cases where the approximation set is clustered, like in MO-HillValLEA, MM-BezEA and Set-BezEA, the average smoothness over all clusters will be taken. In the other cases the smoothness over the entire approximation set is taken.

6.4 Results

The results for all problems and algorithms per indicator can be seen in Table 2.

The HV results clearly show that all algorithms are capable of performing nearly equally in obtaining a good approximation front. However, The MM-BezEA and Set-BezEA algorithms do deteriorate in performance on the MMF1 and 2 problems that have non-linear PSs. The deterioration is inherently caused by the chosen parameterizations that create approximation sets which are linear in shape. Another problem instance where a smaller HV for the new algorithms is obtained, is that of MMF12. Here, despite MM-BezEA obtaining the best PSP values, the approximation sets did not fully approximate the actual PSs and did not cover the endpoints.

The PSP indicator shows similar results, except that MO-RV-GOMEA performs worse as it is not an MMOEA and therefore does not explicitly search for multiple niches. Again promising results for MM-BezEA and Set-BezEA are shown in cases where linear PSs can be found. In the problems with non-linear PSs, MO-HillValLEA and MO_Ring_PSO_SCD manage to find better approximations.

The smoothness results show, as intended, that the chosen parameterizations inherently cause smooth approximation sets. Therefore, MM-BezEA and Set-BezEA always obtain a perfect smoothness of 1.0. Other algorithms do not obtain this, except for MO-RV-GOMEA on 2 of the 11 problems. A visualization of the results of MM-BezEA on the MinDist problem is given in Figure 5. This figure depicts the smooth course of the decision variables in the parallel coordinates plot for the rightmost approximation set in decision space. It contrasts sharply to the parallel coordinates plot of Figure 1.

6.5 Scalability

Set-BezEA has been created to overcome scalability issues with MM-BezEA in highly multi-modal problems. To evaluate this, the OmniTest problem is used, that is scalable in its problem dimensions whilst simultaneously scaling the number of PSs. MM-BezEA and MO-RV-GOMEA will be compared to Set-BezEA with $b \in \{2, 3, 4\}$, to show the impact of requesting more approximation sets. Problem dimensions $\ell \in \{2, 3, 5, 10, 20, 30, 50, 100\}$ have been considered to see how the algorithms behave. The evaluations budget is set to $100000 * \ell$, with the rest of the parameters equal to before.

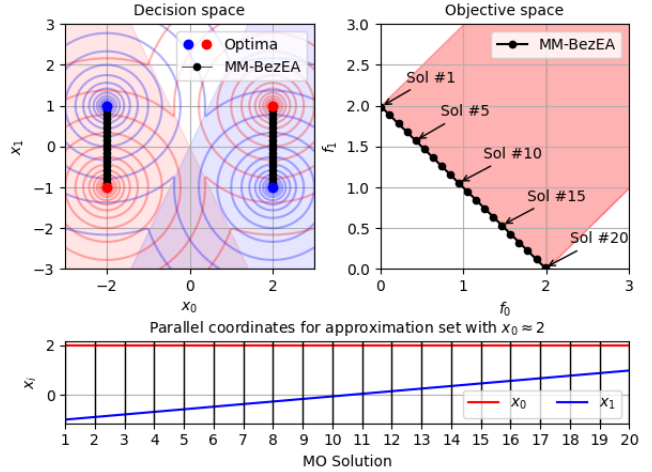


Figure 5: Approximation sets and front with parallel coordinates plot for one of the approximation sets as produced by MM-BezEA on MinDist problem [23].

The PSP metric is omitted, as OmniTest scales very fast in the number of PSs if the problem dimensionality is increased. In case $\ell \geq 8$, there are over 5000 PSs, when only 5000 points of the PSs are analytically determined for the indicators. Thus, only the smoothness and HV indicators are used. Furthermore, as MM-BezEA and Set-BezEA produce approximation sets that are each within a single niche, the approximation set of MO-RV-GOMEA will be post-processed with MO-HVC to compare the average HV per niche.

Figure 6 shows the results for the HV and smoothness indicators. The results show that on average MO-RV-GOMEA seems to obtain reasonable approximation sets within each niche. However, many of these niches have only one or a few solutions, which is also depicted by the lower smoothness values of the entire approximation set on the right. Furthermore, the worst performance in terms of HV per niche can be nearly two orders of magnitude lower than Set-BezEA when $\ell = 100$. MM-BezEA is, like MO-RV-GOMEA, capable of finding a good approximation set for at least one niche as seen by the fact that the best observed performance of all algorithms coincide, but MM-BezEA also has the worst observed performance. For this problem, it is caused by the fact that there are so many niches (3^ℓ), that the algorithm cannot keep track of all of them.

In the case of Set-BezEA, the results indicate that it is capable of finding decent and distinct approximation sets. When more approximation sets are optimized for, the average HV can decline slightly. However, even HV per niche remains high in comparison to the other algorithms, whilst the smoothness stays at its maximum of 1, showing that Set-BezEA exhibits the intended behavior.

7 DISCUSSION

MM-BezEA and Set-BezEA did not cover the endpoints of the PSs in the case of MMF12, which resulted in lower HV values. This can be caused by the fact that the Bézier fitness function will constrain a solution when one of its control points is dominated in objective space by one of the test points. As the endpoints of each part of the discontinuous PF are close to being dominated, i.e., close

Table 2: Results (avg. (\pm st.dev.)) per problem and algorithm over 31 runs, bold identifies best result with statistical significance (Wilcoxon rank-sum test with $\alpha = 0.05$ and Holm-Bonferroni correction).

Indicator	Problem	MM-BezEA	Set-BezEA	MO-HillVallEA	MO_Ring_PSO_SCD	MO-RV-GOMEA	
HV	MinDist	1.17e+02 ($\pm 9.43e-05$)	1.17e+02 ($\pm 3.02e-04$)	1.17e+02 ($\pm 1.62e-02$)	1.17e+02 ($\pm 5.95e-03$)	1.17e+02 ($\pm 1.36e-03$)	
	OmniTest	8.48e+00 ($\pm 2.18e-06$)	8.43e+00 ($\pm 2.34e-01$)	8.47e+00 ($\pm 1.96e-03$)	8.47e+00 ($\pm 7.34e-04$)	8.47e+00 ($\pm 4.82e-04$)	
	Sympart 1	1.17e+02 ($\pm 2.16e-05$)	1.16e+02 ($\pm 1.67e+00$)	1.17e+02 ($\pm 1.42e-02$)	1.17e+02 ($\pm 7.64e-03$)	1.17e+02 ($\pm 1.30e-03$)	
	Sympart 2	1.17e+02 ($\pm 2.91e-05$)	1.15e+02 ($\pm 1.97e+00$)	1.17e+02 ($\pm 7.77e-03$)	1.17e+02 ($\pm 8.75e-03$)	1.17e+02 ($\pm 4.47e-03$)	
	Sympart 3	1.17e+02 ($\pm 9.61e-05$)	1.16e+02 ($\pm 1.76e+00$)	1.17e+02 ($\pm 1.61e-02$)	1.17e+02 ($\pm 9.21e-03$)	1.17e+02 ($\pm 4.91e-03$)	
	TwoOnOne	1.13e+02 ($\pm 1.33e-04$)	1.13e+02 ($\pm 9.27e-04$)	1.13e+02 ($\pm 2.39e-04$)	1.13e+02 ($\pm 1.82e-04$)	1.13e+02 ($\pm 1.10e-04$)	
	MMF 1	6.04e-01 ($\pm 3.86e-02$)	6.29e-01 ($\pm 5.63e-02$)	8.05e-01 ($\pm 2.37e-04$)	8.05e-01 ($\pm 8.69e-05$)	8.05e-01 ($\pm 6.60e-05$)	
	MMF 2	6.34e-01 ($\pm 2.01e-04$)	5.88e-01 ($\pm 9.42e-02$)	8.04e-01 ($\pm 6.90e-04$)	8.04e-01 ($\pm 9.59e-04$)	8.05e-01 ($\pm 1.75e-04$)	
	MMF 12	1.78e+00 ($\pm 2.02e-06$)	1.38e+00 ($\pm 2.02e-01$)	2.06e+00 ($\pm 2.57e-03$)	2.06e+00 ($\pm 2.05e-03$)	2.06e+00 ($\pm 1.49e-04$)	
	MMF 14	5.63e+00 ($\pm 1.33e-05$)	5.63e+00 ($\pm 6.40e-03$)	5.63e+00 ($\pm 7.26e-04$)	5.63e+00 ($\pm 1.92e-03$)	5.63e+00 ($\pm 2.23e-04$)	
	MMF 15	5.56e+00 ($\pm 2.03e-02$)	5.56e+00 ($\pm 4.47e-03$)	5.57e+00 ($\pm 6.52e-04$)	5.56e+00 ($\pm 1.54e-03$)	5.57e+00 ($\pm 1.79e-04$)	
	PSP	MinDist	3.26e+02 ($\pm 7.31e+01$)	3.77e+02 ($\pm 9.41e+01$)	5.02e+01 ($\pm 2.74e+00$)	6.97e+01 ($\pm 6.73e+00$)	1.21e+00 ($\pm 1.65e+00$)
		OmniTest	2.36e+02 ($\pm 8.81e+01$)	1.71e-02 ($\pm 3.34e-02$)	7.13e+01 ($\pm 2.76e+00$)	6.90e+01 ($\pm 9.56e+00$)	1.36e-01 ($\pm 2.43e-01$)
		Sympart 1	2.67e+02 ($\pm 1.21e+02$)	1.22e-03 ($\pm 2.89e-03$)	3.56e+01 ($\pm 1.57e+00$)	2.79e+01 ($\pm 3.69e+00$)	1.16e-02 ($\pm 2.70e-02$)
		Sympart 2	3.09e+02 ($\pm 8.46e+01$)	2.76e-04 ($\pm 3.54e-04$)	3.60e+01 ($\pm 7.42e-01$)	2.38e+01 ($\pm 2.46e+00$)	1.02e-02 ($\pm 1.71e-02$)
Sympart 3		6.41e+01 ($\pm 7.77e+01$)	1.27e-03 ($\pm 2.17e-03$)	4.33e+01 ($\pm 2.10e+00$)	2.64e+01 ($\pm 5.62e+00$)	8.09e-03 ($\pm 1.33e-02$)	
TwoOnOne		3.04e+02 ($\pm 2.18e+02$)	2.69e+02 ($\pm 1.15e+02$)	4.50e+01 ($\pm 7.21e-01$)	2.45e+01 ($\pm 1.03e+01$)	2.68e+00 ($\pm 1.11e+00$)	
MMF 1		7.22e+00 ($\pm 2.41e+00$)	4.56e-01 ($\pm 3.55e-01$)	3.17e+01 ($\pm 6.84e-01$)	3.80e+01 ($\pm 6.79e+00$)	1.02e+00 ($\pm 2.89e-01$)	
MMF 2		4.00e+00 ($\pm 2.49e+00$)	4.29e-02 ($\pm 5.23e-02$)	1.17e+02 ($\pm 1.21e+01$)	5.04e+01 ($\pm 1.51e+01$)	2.18e+00 ($\pm 1.41e+00$)	
MMF 12		2.42e+01 ($\pm 7.72e+00$)	4.83e-01 ($\pm 6.81e-01$)	1.94e+01 ($\pm 6.46e+00$)	1.53e+01 ($\pm 1.46e-01$)	8.67e+00 ($\pm 1.36e+00$)	
MMF 14		2.68e+03 ($\pm 4.82e+02$)	1.72e+03 ($\pm 1.60e+03$)	3.70e+02 ($\pm 1.03e+01$)	2.31e+02 ($\pm 2.16e+01$)	1.08e+00 ($\pm 2.84e+00$)	
MMF 15		2.73e+02 ($\pm 4.17e+02$)	2.96e+02 ($\pm 1.41e+02$)	2.65e+02 ($\pm 4.58e+00$)	2.44e+02 ($\pm 7.25e+00$)	2.24e+01 ($\pm 1.40e-02$)	
Smoothness		MinDist	1.00e+00 ($\pm 0.00e+00$)	1.00e+00 ($\pm 0.00e+00$)	8.09e-01 ($\pm 3.70e-02$)	7.63e-01 ($\pm 5.91e-03$)	8.94e-01 ($\pm 1.81e-01$)
		OmniTest	1.00e+00 ($\pm 0.00e+00$)	1.00e+00 ($\pm 0.00e+00$)	9.23e-01 ($\pm 5.65e-03$)	7.28e-01 ($\pm 9.76e-03$)	7.16e-01 ($\pm 1.96e-01$)
		Sympart 1	1.00e+00 ($\pm 0.00e+00$)	1.00e+00 ($\pm 0.00e+00$)	8.76e-01 ($\pm 2.52e-02$)	6.84e-01 ($\pm 9.76e-03$)	7.01e-01 ($\pm 2.09e-01$)
		Sympart 2	1.00e+00 ($\pm 0.00e+00$)	1.00e+00 ($\pm 0.00e+00$)	8.78e-01 ($\pm 2.14e-02$)	5.73e-01 ($\pm 9.30e-03$)	7.87e-01 ($\pm 1.68e-01$)
	Sympart 3	1.00e+00 ($\pm 0.00e+00$)	1.00e+00 ($\pm 0.00e+00$)	8.70e-01 ($\pm 3.10e-02$)	5.29e-01 ($\pm 1.18e-02$)	8.30e-01 ($\pm 1.92e-01$)	
	TwoOnOne	1.00e+00 ($\pm 0.00e+00$)	1.00e+00 ($\pm 0.00e+00$)	7.77e-01 ($\pm 1.21e-02$)	7.47e-01 ($\pm 9.36e-03$)	7.51e-01 ($\pm 1.59e-01$)	
	MMF 1	1.00e+00 ($\pm 0.00e+00$)	1.00e+00 ($\pm 0.00e+00$)	9.01e-01 ($\pm 3.98e-02$)	7.82e-01 ($\pm 8.49e-03$)	5.86e-01 ($\pm 9.13e-02$)	
	MMF 2	1.00e+00 ($\pm 0.00e+00$)	1.00e+00 ($\pm 0.00e+00$)	9.38e-01 ($\pm 1.26e-02$)	5.01e-01 ($\pm 8.92e-03$)	8.46e-01 ($\pm 1.60e-01$)	
	MMF 12	1.00e+00 ($\pm 0.00e+00$)	1.00e+00 ($\pm 0.00e+00$)	8.35e-01 ($\pm 2.73e-02$)	6.35e-01 ($\pm 9.86e-03$)	1.00e+00 ($\pm 0.00e+00$)	
	MMF 14	1.00e+00 ($\pm 0.00e+00$)	1.00e+00 ($\pm 0.00e+00$)	9.31e-01 ($\pm 1.17e-02$)	8.71e-01 ($\pm 1.11e-02$)	9.62e-01 ($\pm 1.05e-01$)	
	MMF 15	1.00e+00 ($\pm 0.00e+00$)	1.00e+00 ($\pm 0.00e+00$)	9.19e-01 ($\pm 1.43e-02$)	8.63e-01 ($\pm 8.54e-03$)	1.00e+00 ($\pm 0.00e+00$)	

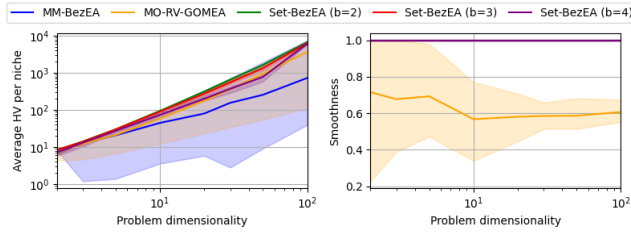


Figure 6: Results of dimensionality approximation. The left diagram shows the HV results, with the approximation set smoothness on the right. The averages are depicted as a line and the min. and max. values as shaded areas over 31 runs. MM-BezEA and Set-BezEA smoothness results overlap.

to the constraint space, it can lead to not entirely capturing the discontinuous pieces of the PF and thus resulting in a lower HV.

The use of the HV indicator to score individuals in MM-BezEA and Set-BezEA is useful in the sense that it is a Pareto compliant indicator [14, 37], but it does suffer from a downside. In some situations the endpoints of the approximation sets cannot reach the endpoints of the Pareto set [3]. Even in cases where the number of test points will be set to infinity, the reference point can never be set so that the extremes are captured.

Even though the smoothness indicator tries to determine whether an approximation set is smooth by measuring the detour length, it comes down to determining the angle between solutions. This implies that it only considers linear curves to be perfectly smooth. If an approximation set oscillates slightly around a PS, the angles between solutions will therefore result in a lower smoothness. In

cases where the niches can be separated in a good manner, another definition of smoothness that considers the oscillation around the PS might be more useful.

Future work could investigate the further use of the Bézier parameterizations with more control points to approximate non-linear Pareto sets. Furthermore, Bézier simplexes [19] might be usable for problems with more than two objectives.

8 CONCLUSION

We proposed two algorithms, MM-BezEA and Set-BezEA, to search for parameterizations of approximation sets that define smooth curves in the decision space for bi-objective optimization problems. In highly multi-modal problems, good navigability of approximation sets is desired by decision makers, which can be further improved if approximation sets for a specific number of modes can be requested. The results show that the smoothness is indeed enforced by the Bézier parameterizations. Furthermore, the encoding of b curves in Set-BezEA produces an exact number of approximation sets that are of high quality for highly multi-modal problems. Both algorithms were outperformed in problems with non-linear Pareto sets, but only low-order Bézier curves were researched. If the non-linearity of a mode surpasses the Bézier order, it can no longer be captured by the Bézier curve. All together, the algorithms are still potentially very useful in practice, which will be targeted in future work.

ACKNOWLEDGMENTS

Leah R.M. Dickhoff was supported by the Dutch Cancer Society (KWF kankerbestrijding, Project N.12183) and Elekta.

REFERENCES

- [1] Ali Ahrari, Kalyanmoy Deb, and Mike Preuss. 2017. Multimodal Optimization by Covariance Matrix Self-Adaptation Evolution Strategy with Repelling Subpopulations. *Evolutionary Computation* 25, 3 (Sep 2017), 439–471. https://doi.org/10.1162/evco_a_00182
- [2] Tanja Alderliesten, Peter A. N. Bosman, and Arjan Bel. 2015. Getting the most out of additional guidance information in deformable image registration by leveraging multi-objective optimization. In *Medical Imaging 2015: Image Processing*, Vol. 9413. SPIE, Bellingham, WA, USA, 469–475. <https://doi.org/10.1117/12.2081438>
- [3] Anne Auger, Johannes Bader, Dimo Brockhoff, and Eckart Zitzler. 2009. Theory of the Hypervolume Indicator: Optimal μ -Distributions and the Choice of the Reference Point. In *Proceedings of the tenth ACM SIGEVO workshop on Foundations of genetic algorithms* (Orlando, Florida, USA) (FOGA '09). Association for Computing Machinery, New York, NY, USA, 87–102. <https://doi.org/10.1145/1527125.1527138>
- [4] Anne Auger and Nikolaus Hansen. 2005. A restart CMA evolution strategy with increasing population size. In *2005 IEEE Congress on Evolutionary Computation*, Vol. 2. IEEE, New York, NY, USA, 1769–1776. Vol. 2. <https://doi.org/10.1109/CEC.2005.1554902>
- [5] Rudolf Berghammer, Tobias Friedrich, and Frank Neumann. 2012. Convergence of set-based multi-objective optimization, indicators and deteriorative cycles. *Theoretical Computer Science* 456 (Oct 2012), 2–17. <https://doi.org/10.1016/j.tcs.2012.05.036>
- [6] Nicola Beume, Boris Naujoks, and Michael Emmerich. 2007. SMS-EMOA: Multiobjective selection based on dominated hypervolume. *European Journal of Operational Research* 181, 3 (Sep 2007), 1653–1669. <https://doi.org/10.1016/j.ejor.2006.08.008>
- [7] Peter A.N. Bosman. 2010. The Anticipated Mean Shift and Cluster Registration in Mixture-Based EDAs for Multi-Objective Optimization. In *Proceedings of the 12th Annual Conference on Genetic and Evolutionary Computation* (Portland, Oregon, USA) (GECCO '10). Association for Computing Machinery, New York, NY, USA, 351–358. <https://doi.org/10.1145/1830483.1830549>
- [8] Anton Bouter, Tanja Alderliesten, Cees Witteveen, and Peter A. N. Bosman. 2017. Exploiting Linkage Information in Real-Valued Optimization with the Real-Valued Gene-Pool Optimal Mixing Evolutionary Algorithm. In *Proceedings of the Genetic and Evolutionary Computation Conference* (Berlin, Germany) (GECCO '17). Association for Computing Machinery, New York, NY, USA, 705–712. <https://doi.org/10.1145/3071178.3071272>
- [9] Anton Bouter, Ngoc Hoang Luong, Cees Witteveen, Tanja Alderliesten, and Peter A. N. Bosman. 2017. The Multi-Objective Real-Valued Gene-Pool Optimal Mixing Evolutionary Algorithm. In *Proceedings of the Genetic and Evolutionary Computation Conference* (Berlin, Germany) (GECCO '17). Association for Computing Machinery, New York, NY, USA, 537–544. <https://doi.org/10.1145/3071178.3071274>
- [10] Paul Darwen and Xin Yao. 1995. A dilemma for fitness sharing with a scaling function. In *Proceedings of 1995 IEEE International Conference on Evolutionary Computation*, Vol. 1. IEEE, New York, NY, USA, 166–171. <https://doi.org/10.1109/ICEC.1995.489138>
- [11] Kalyanmoy Deb. 2000. An efficient constraint handling method for genetic algorithms. *Computer Methods in Applied Mechanics and Engineering* 186, 2 (Jun 2000), 311–338. [https://doi.org/10.1016/S0045-7825\(99\)00389-8](https://doi.org/10.1016/S0045-7825(99)00389-8)
- [12] Kalyanmoy Deb. 2001. *Multi-Objective Optimization Using Evolutionary Algorithms*. John Wiley & Sons, Inc., USA.
- [13] Kalyanmoy Deb and Santosh Tiwari. 2008. Omni-optimizer: A generic evolutionary algorithm for single and multi-objective optimization. *European Journal of Operational Research* 185, 3 (Mar 2008), 1062–1087. <https://doi.org/10.1016/j.ejor.2006.06.042>
- [14] Mark Fleischer. 2003. The Measure of Pareto Optima Applications to Multi-Objective Metaheuristics. In *Proceedings of the 2nd International Conference on Evolutionary Multi-Criterion Optimization* (Faro, Portugal) (EMO'03). Springer-Verlag, Berlin, Heidelberg, 519–533.
- [15] David E. Goldberg, Kalyanmoy Deb, and Jeffrey Horn. 1992. Massive Multimodality, Deception, and Genetic Algorithms. In *Parallel Problem Solving from Nature 2* (Brussels, Belgium) (PPSN-2). Elsevier Science Publishers B. V., Amsterdam, The Netherlands, The Netherlands, 37–48.
- [16] Ilan Gronau and Shlomo Moran. 2007. Optimal implementations of UPGMA and other common clustering algorithms. *Inform. Process. Lett.* 104, 6 (Dec 2007), 205–210. <https://doi.org/10.1016/j.ipl.2007.07.002>
- [17] Andrea P. Guerreiro, Carlos M. Fonseca, and Luís Paquete. 2016. Greedy Hypervolume Subset Selection in Low Dimensions. *Evolutionary Computation* 24 (Sep 2016), 521–544. Issue 3. https://doi.org/10.1162/evco_a_00188
- [18] John H. Holland. 1975. *Adaptation in Natural and Artificial Systems: An Introductory Analysis with Applications to Biology, Control, and Artificial Intelligence*. University of Michigan Press, Ann Arbor, MI, USA.
- [19] Ken Kobayashi, Naoki Hamada, Akiyoshi Sannai, Akinori Tanaka, Kenichi Bannai, and Masashi Sugiyama. 2019. Bézier simplex fitting: Describing pareto fronts of simplicial problems with small samples in multi-objective optimization. In *Proceedings of the 33rd AAAI Conference on Artificial Intelligence, AAAI 2019, the 31st Innovative Applications of Artificial Intelligence Conference, IAAI 2019 and the 9th AAAI Symposium on Educational Advances in Artificial Intelligence, EAAI 2019* (Honolulu, Hawaii, USA). AAAI press, Palo Alto, CA, USA, 2304–2313.
- [20] Xiaodong Li, Michael G. Epitropakis, Kalyanmoy Deb, and Andries Engelbrecht. 2017. Seeking Multiple Solutions: An Updated Survey on Niching Methods and Their Applications. *IEEE Transactions on Evolutionary Computation* 21, 4 (Aug 2017), 518–538. <https://doi.org/10.1109/TEVC.2016.2638437>
- [21] Jing Liang, Boyang Qu, Dunwei Gong, and Cai Yue. 2018. *Problem Definitions and Evaluation Criteria for the CEC 2019 Special Session on Multimodal Multiobjective Optimization*. Technical Report. <https://doi.org/10.13140/RG.2.2.33423.64164>
- [22] Samir W. Mahfoud. 1996. *Niching Methods for Genetic Algorithms*. Ph. D. Dissertation. University of Illinois at Urbana-Champaign, USA. UMI Order No. GAX95-43663.
- [23] Stefanus C. Maree, Tanja Alderliesten, and Peter A. N. Bosman. 2019. Real-Valued Evolutionary Multi-Modal Multi-Objective Optimization by Hill-Valley Clustering. In *Proceedings of the Genetic and Evolutionary Computation Conference* (Prague, Czech Republic) (GECCO '19). Association for Computing Machinery, New York, NY, USA, 568–576. <https://doi.org/10.1145/3321707.3321759>
- [24] Stefanus C. Maree, Tanja Alderliesten, and Peter A. N. Bosman. 2020. Ensuring Smoothly Navigable Approximation Sets by Bézier Curve Parameterizations in Evolutionary Bi-objective Optimization. In *Parallel Problem Solving from Nature – PPSN XVI*. Springer International Publishing, Cham, 215–228.
- [25] Stefanus C. Maree, Tanja Alderliesten, and Peter A. N. Bosman. 2021. Uncrowded Hypervolume-based Multi-objective Optimization with Gene-pool Optimal Mixing. *Evolutionary Computation* (Dec 2021), 1–24. https://doi.org/10.1162/evco_a_00303
- [26] Stefanus C. Maree, Tanja Alderliesten, Dirk Thierens, and Peter A. N. Bosman. 2018. Real-Valued Evolutionary Multi-Modal Optimization Driven by Hill-Valley Clustering. In *Proceedings of the Genetic and Evolutionary Computation Conference* (Kyoto, Japan) (GECCO '18). Association for Computing Machinery, New York, NY, USA, 857–864. <https://doi.org/10.1145/3205455.3205477>
- [27] Mike Preuss. 2010. Niching the CMA-ES via Nearest-Better Clustering. In *Proceedings of the 12th Annual Conference Companion on Genetic and Evolutionary Computation* (Portland, Oregon, USA) (GECCO '10). Association for Computing Machinery, New York, NY, USA, 1711–1718. <https://doi.org/10.1145/1830761.1830793>
- [28] Mike Preuss, Boris Naujoks, and Günter Rudolph. 2006. Pareto Set and EMOA Behavior for Simple Multimodal Multiobjective Functions. In *Parallel Problem Solving from Nature – PPSN IX* (Reykjavik, Iceland) (PPSN'06). Springer-Verlag, Berlin, Heidelberg, 513–522. https://doi.org/10.1007/11844297_52
- [29] Günter Rudolph, Boris Naujoks, and Mike Preuss. 2006. Capabilities of EMOA to Detect and Preserve Equivalent Pareto Subsets. In *Evolutionary Multi-Criterion Optimization, 4th International Conference, EMO 2007, Matsushima, Japan, March 5-8, 2007, Proceedings (Lecture Notes in Computer Science, Vol. 4403)*. Springer, Berlin, Heidelberg, 36–50. https://doi.org/10.1007/978-3-540-70928-2_7
- [30] Dirk Thierens. 2010. The Linkage Tree Genetic Algorithm. In *Proceedings of Parallel Problem Solving from Nature, PPSN XI* (Berlin, Heidelberg) (Lecture Notes in Computer Science). Springer, Berlin, Heidelberg, 264–273.
- [31] Ye Tian, Ran Cheng, Xingyi Zhang, and Yaochu Jin. 2017. PlatEMO: A MATLAB platform for evolutionary multi-objective optimization. *IEEE Computational Intelligence Magazine* 12, 4 (Nov 2017), 73–87.
- [32] Cheikh Touré, Nikolaus Hansen, Anne Auger, and Dimo Brockhoff. 2019. Uncrowded Hypervolume Improvement: COMO-CMA-ES and the Sofomore Framework. In *Proceedings of the Genetic and Evolutionary Computation Conference* (Prague, Czech Republic) (GECCO '19). Association for Computing Machinery, New York, NY, USA, 638–646. <https://doi.org/10.1145/3321707.3321852>
- [33] R.K. Ursem. 1999. Multinational evolutionary algorithms. In *Proceedings of the 1999 Congress on Evolutionary Computation-CEC99*, Vol. 3. IEEE, New York, NY, USA, 1633–1640. Vol. 3. <https://doi.org/10.1109/CEC.1999.785470>
- [34] Cai Yue, Boyang Qu, and Jing Liang. 2017. A Multi-objective Particle Swarm Optimizer Using Ring Topology for Solving Multimodal Multi-objective Problems. *IEEE Transactions on Evolutionary Computation* 22 (Sep 2017), 805–817. <https://doi.org/10.1109/TEVC.2017.2754271>
- [35] Qingfu Zhang and Hui Li. 2007. MOEA/D: A Multiobjective Evolutionary Algorithm Based on Decomposition. *IEEE Transactions on Evolutionary Computation* 11 (12 2007), 712–731. Issue 6. <https://doi.org/10.1109/TEVC.2007.892759>
- [36] Eckart Zitzler and Lothar Thiele. 1999. Multiobjective evolutionary algorithms: a comparative case study and the strength Pareto approach. *IEEE Transactions on Evolutionary Computation* 3, 4 (Nov 1999), 257–271. <https://doi.org/10.1109/4235.797969>
- [37] Eckart Zitzler, Lothar Thiele, Marco Laumanns, Carlos M. Fonseca, and Viviane G. da Fonseca. 2003. Performance assessment of multiobjective optimizers: an analysis and review. *IEEE Transactions on Evolutionary Computation* 7, 2 (May 2003), 117–132. <https://doi.org/10.1109/TEVC.2003.810758>